J Intell Robot Syst (2015) 78:401–423
DOI 10.1007/s10846-014-0067-0

Terrain Classification and Negotiation with a Walking Robot

Krzysztof Walas

Received: 9 September 2013 / Accepted: 20 May 2014 / Published online: 12 July 2014

Abstract This paper describes a walking robot controller for negotiation of terrains with different traction characteristics. The feedback is based on three perception systems. The purpose of the presented research is to enhance the autonomy of the walking robot. The information about the class of the terrain allows the robot to work in the real world scenarios more efficiently. In the presented work twelve types of the ground were tested. Suitability of each type of the perception system for characterizing the terrain class was checked. Namely, vision, depth and tactile sensors were used. In each case as a classifier the Support Vector Machines were utilized. The separate classification results from each sensor were combined to obtain better precision and recall in the ground classification process. The information about the terrain type was fed into robot controller to adapt the robot gait parameters. The goal was to achieve good balance between the speed of the movement and the vibration caused by the bounciness and the irregularities of the terrain.

The paper begins with the description of the experimental setup. Next, the classification results for each sensor used are presented. Then, the rules of combining classifiers were tested. Finally, the robot gait controller was proposed and evaluated.

Keywords Walking robots · Terrain classification · Gait control

1 Introduction

Walking robot to operate in a real world scenarios requires the knowledge about the terrain type which it is going to negotiate. This information is indispensable for adjusting the gait characteristics to the ground type. Using the appropriate gait parameters allows the robot to walk reliably and efficiently on different surfaces. Walking robots which control systems takes into account the information about the properties of the terrain are scarce. However, there are many examples of the perception systems for obtaining the information about the terrain class. This knowledge could be gathered using different sensors: cameras, depth sensors, Inertial Measurements Units or Force/Torque sensors. In literature examples of the use of each type of the sensing modality for ground classification purposes were described.

The author gratefully acknowledge the support from the Polish National Science Centre, Grant No. 2011/01/N/ST7/02070.

Parts of this work have been presented at ([43]); that work did not present how the results of the classifiers were merged and how the experiments to obtain the controller were performed.

K. Walas (✉)
Poznan University of Technology, Poznan, Poland
e-mail: krzysztof.walas@put.poznan.pl

1.1 Related Work

Visual Perception The most popular sensor in robotics is a camera. Research on vision systems is well developed and many algorithms for image processing are available. The use of machine vision for the ground classification is described in several papers. The group from Oxford is working on visual urban scene labelling [32, 36]. The purpose of their research is to equip the autonomous car with the reliable perception system of the surroundings. The investigation is mainly focused on urban environment. Research described in [1] is concentrated on the natural environment. Authors have taken into account the intra-class variability of the selected terrains and use hierarchical classifiers to lower the cost of the computation. In [13] visual classification of the ground type was used to change the gait patterns of the Little Dog robot.

Depth Perception The topic closely related to the computer vision is depth sensing. In most cases, for the task of the terrain classification, the robots are equipped with camera and the information obtained from images is supported by the depth data. This is the case for DARPA challenge robotic cars [39], as well as for the robotic cars build in UK [36]. There are also projects where only the depth sensor is used for a navigation and recognition of the ground type. For example planetary rover described in [14] or Unmanned Ground Vehicle (UGV) presented in [28].

Tactile Perception Different approach to gathering information about the ground is the use of Inertial Measurement Unit (IMU) or Force/Torque (F/T) sensor. Majority of the research on this topic is done for the mobile, wheeled platforms equipped with IMU [7, 34, 47]. In the experiments described in the above-mentioned papers vibrations of the robot chassis while riding on different terrain types were measured. The registered signals were used for the classification purposes. Authors of [15–17] are presenting similar approach but they are using a simple tactile probe, equipped with an accelerometer, for the terrain classification. Other method of material classification was reported in [26]. The dynamic tactile sensor – compliant pin that makes contact with the surface, and a capacitor microphone form a sensing device. The classification is based on mixed visual and tactile information. Other example of applying two types of measurements (vibrations and vision) to terrain classification process was described in [48].

In the field of walking robots one approach to sensing the ground could be the use of inertial measurements and joint currents in robot leg, as it was presented in [4]. The description of the vibration based terrain classification using single robot leg was given in [20]. The method was further extended to natural terrains and presented in [19]. The perception of the ground based on the measurements of the forces and torques at the tip of the robotic leg during the single step is described in our earlier work [42, 46].

Rough Terrain Negotiation The research on motion of the multi-legged walking robots is mainly focused on the roughness of the terrain – its relief. For example in DARPA Locomotion Challenge the algorithms for terrain negotiation were tested on the ground mock-up [24]. Other research which was focused on the terrain shape was presented in [3]. Nonetheless, there are some research done where the type of the ground is taken into account in the gait control algorithm. One of the examples could be [18], where the robot RHex is able to identify if it is either walking on the dry or wet sand and it is either in the water or not. The robot selects the appropriate gait accordingly. This research was further extended to other terrain types and walking speed adaptation in [31]. Other recent research on recognizing terrain type is presented in [4]. These two aforementioned approaches are based on the tactile information and are rather limited in the range of the terrain types which were used in the experiments. Namely, there were respectively only four and three types of the terrains used in the tests. In the work described in [13] the classification is based on the vision information and the performance of the robot was tested for five ground types using three preprogrammed gaits. Similar approach to the aforementioned one was presented in [50]. Some advances in six-legged robot gait control were described in [35], where the robot was able to adjust to the irregularities of the terrain dynamically using the information about the contact with the ground. However, the presented results regarded only ground relief. Additionally, some simulation work was done on the cost of locomotion of the hexapod robot [49].

Apart from the multi-legged robots some research in the terrain negotiation is done for the biped robots. For example the simulation on the ground compliance

were performed for the robot SHERPA [11]. On the other hand some similar research was done using adjustable stiffness of the robot leg [40]. The research on the influence of the ground type on the gait is also conducted in the study of the human walking as for example in [29, 30].

In the presented paper the Discrete Event Systems (DES) approach was used for the control of the robot. Such an approach was proposed as early as at the end of 80's in [8]. The further work on this topic is described in [21]. The DES approach was used for obstacle avoidance [23] and gait generation for multi-limbed robots [33]. The graph approach to rock climbing performed by the robot was proposed in [6]. The latest research in the field of walking robots is mainly focused on hybrid systems. The attempts of using this mathematical apparatus are presented in [9]. The more extended approach is described in [37] where the hybrid system was used for achieving robotic bipedal walking. Our earlier paper [45] also describes the use of DES for urban obstacles negotiation.

1.2 Approach

Our first contribution is the use of the larger dataset of the ground samples – 12 – comparing to the similar research done for the walking robots and known to the author. In relation to [4, 18] our set is 4 times larger and comparing to [13] where 6 terrain types were tested our database is two times larger. The largest set of terrain samples – 8 – were tested in the experiments conducted with the walking robot and described in [50].

Moreover, the classification was performed by simultaneously using three types of perception systems i.e. RGB, depth and tactile. Such an approach has not been yet encountered by the author in the literature regarding walking robots. What is more, the rule for combining the results of the separate classifiers suitable for the task was proposed. The gain of the discriminative power of the classifier resulting from the use of each sensing modality was checked. Based on this results, combined visual-tactile sensing, data acquisition scenario was introduced.

Additionally, the controller which is adjusting walking robot gait parameters to the terrain type using DES was proposed.

The reminder of the paper is the following. At the beginning the experimental setup is described. Then, the classification results for each sensing modality are presented. Next, the proposed approach to merging the results from separate classifiers is given. Subsequently, the influence of the gait parameters on the robot performance while walking on the different terrain types is shown. Then, the robot gait controller is proposed and evaluated. At the end concluding remarks are given.

2 Experimental Setup

2.1 Walking Robot

In our experiments, the six-legged walking robot called Messor was used. The trunk of the robot is 30.6 cm long and 26 cm wide. The segments of the leg have the following dimensions (looking from the trunk of the robot): coxa 5.5 cm, femur 16 cm, tibia 23 cm. The servomotors in the leg joints are position controlled. The robot is equipped with Hitec HSR-5990TG with HMI (Hitec Multi-protocol Interface) which allows only to change P and D gain of the internal controller, using three fixed values. However, the speed of the motor rotation could be set in the wider range of values. The robot is shown in Fig. 1 and it is described in details in [44].

For the purposes of the ground classification the Kinect RGB-D sensor and Force/Torque sensor (ATI Mini-45) mounted on the tip of the robot leg were used. Additionally, on the chassis of the robot, approximately in its centre of mass, the Attitude Heading

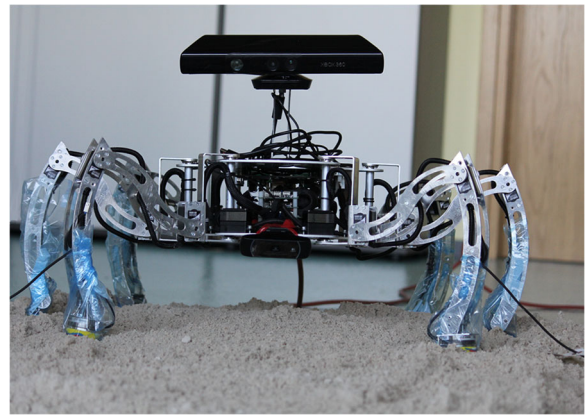

Fig. 1 Messor walking robot used in the experiments

Reference System (AHRS) Xsens MT-28A53G25 is mounted.

In the controller evaluation process video camera uEye-UI-1225LE-C was utilized. It has a picture resolution of 752x482 px and frame rate 87 fps.

2.2 Experimental Mockup

For the experiments twelve types of the terrain were prepared. The robot was walking on: artificial grass, grit, pebbles, sand, green rubber tiles, concrete ground, black rubber tiles, wooden boards, rocks, PVC tiles, ceramic tiles and carpet tiles. All the ground types are shown in Fig. 2. The selected terrain samples are frequently encountered indoors and outdoors. Some of the terrain classes in the set are hardly distinguishable for one type of the perception system, but are easy to differentiate by the other type. For example: green and black rubber tile are easily distinguishable by the vision system, but they have the same shape – depth sensor, or the same bounciness – tactile sensor. On the other hand pebbles and ceramic tiles have the same texture, but different shape and different bounciness.

2.3 Software Used

To perform most of our research we were using off-the-shelf libraries. For the machine vision algorithms the OpenCV library [5] was used. For managing point clouds the Point Cloud Library was utilized [38]. Classification problems were solved using SVMLIB [10].

3 Terrain Classification

3.1 Depth Perception

The description of the terrain in the spatial context provides useful features for the ground classification process. Its shape gives the information of the height of the obstacles as well as of the terrain roughness and irregularities.

Data Acquisition For depth data acquisition Microsoft Kinect was used. Registration was performed in changing lighting conditions. The data was acquired in the laboratory in the daylight (the sunlight was passing through the side windows of the room) and with the artificial light (fluorescent). The Kinect device was moved around the terrain samples. The snapshots were taken about 40 cm above the ground and the camera was tilted down as it is shown in Fig. 3. From each point cloud of the terrain small patch was taken (10x10 cm).

The data was acquired without using the IMU. Therefore, the orientation of the patch local coordinates frame regarding to the global reference frame attached to the ground had to be established. In order to do so, the normal to the surface for the centroid of the patch was calculated. Radius for obtaining the normal to the surface was set to 5 cm – to obtain averaged value. Next, the patch was translated and the centroid of the patch was aligned with the origin of the global reference frame. Then, the patch was rotated so the majority of the normals points upwards. The obtained rotation was not accurate, so using the

Fig. 2 Terrain types used in experiments: artificial grass **a**, grit **b**, pebbles **c**, sand **d**, green rubber tiles **e**, concrete ground **f**, black rubber tiles **g**, wooden boards **h**, rocks **i**, PVC tiles **j**, ceramic tiles **k** and carpet tiles **l**

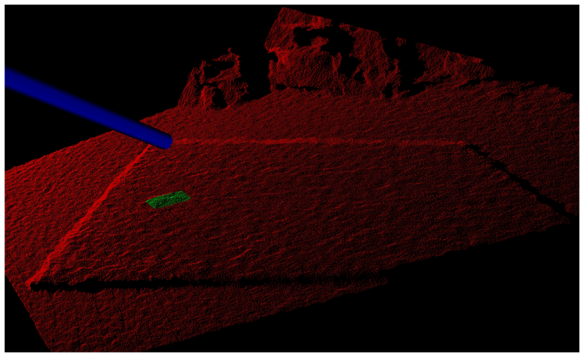

Fig. 3 Patch of the point cloud registered during the experiments

Iterative Closest Point method the patch was rotated and the local coordinates frame was aligned with global reference frame.

Features Having the appropriately prepared patch of the point cloud the set of features was proposed. For each dimension (x,y,z) the standard deviation for the position of all the points was calculated. Next, the standard deviation of all the normal vectors components (x,y,z) was calculated (with radius of 1 cm). Feature descriptor for each patch has six dimensions.

$$x_{pc} = [std(X), std(Y), std(Z), std(N_x), std(N_y), std(N_z)] \quad (1)$$

where:
$\mathbf{x_{pc}}$ – feature vector for the point cloud;
X, Y, Z – position of the points $\mathbf{p_i}$;
N_x, N_y, N_z – components of the normal vectors $\mathbf{n_i}$;
$i = 1 \ldots m$, where m is the number of points in the cloud patch.

The selection of the features is based on related work on that subject. In [22] terrain roughness index was proposed. It is calculated as a standard deviation of local elevations. Additionally, the terrain classification described in [28] was performed with the covariance matrix computed for the distribution of 3D points. Moreover, the approach based on calculating normals was described in [2]. It is named Unevenness Point Descriptor (UPD). The equation for UPD contains module of the sum of the normal vectors in the selected point neighbourhood. This provides the invariance to the terrain slope. Likewise, the influence of the terrain slope could be alleviated by first calculating the ground plain and then transforming it to the common reference frame as it was presented in [27]. Then, the standard deviation of point height is invariant to the slope of the terrain and the set of features selected in the presented research could be used. However, in the approach presented in this paper fixed orientation of the ground plain was assumed for all terrain samples.

Results During the data acquisition phase 84 patches for each terrain sample were gathered. The data was split into two sets: training (60 patches) and testing (24 patches). The described above feature vectors were passed to the SVM classifier. The classifier was trained to identify 12 classes of the terrain (see Fig. 2). The parameters of the SVM were established using grid search and the cross-validation. The best precision for the training set was equal to 63.33 %. The classification result for the testing set was worse and was equal to 51.90 %. The confusion matrix for the classification of testing data is shown in Fig. 4.

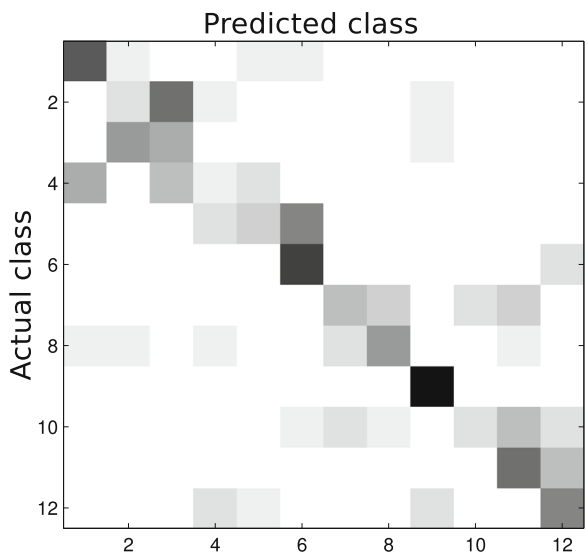

Fig. 4 Confusion matrix for classification of 12 terrain types using point cloud data. Classes names are: artificial grass(1), grit(2), pebbles(3), sand(4), green rubber tiles(5), concrete ground(6), black rubber tiles(7), wooden boards(8), rocks(9), PVC tiles(10), ceramic tiles(11) and carpet tiles(12)

3.2 Tactile Perception

Other sensor which enables the acquisition of the data about the characteristics of the ground is the F/T sensor mounted on the robot foot. The force and torque signals are measured while robot is walking on the different ground types. The obtained data is used to solve the classification problem.

Data Acquisition Data were gathered by using ATI Mini-45 sensor, which is calibrated by the manufacturer. Robot was walking straight with the average walking speed V = 2 cm/s, using wave gait. The measurements are acquired during the whole motion of the robot, in static and dynamic states. The sampling frequency of the transducer was set to 200 Hz. The obtained signal comprise 400 samples for each robot step. For each ground sample data from 42 steps was acquired. The data consists of 6 channels, 3 force vector components (F_x, F_y, F_z) and 3 torque vector components (T_x, T_y, T_z). The exemplary signals from the transducer, acquired while robot was walking on the rocks, is shown in Fig. 5. The force and torque data were shown on separate plots due to its different scale. Each colour on the plot represents different component of the force and torque vector. Namely, red – x, green – y, blue – z.

Features To obtain the features appropriate for the classification, the approach similar to the one presented in [17, 47] was adopted. Namely, the four different statistical values of the registered signals were computed – variance, skewness, kurtosis and the 5th statistical moment.

$$\mathbf{x_{tc}} = [var(F_x), skew(F_x), kurt(F_x), \mu_5(F_x), \ldots, var(T_z), skew(T_z), kurt(T_z), \mu_5(T_z)] \quad (2)$$

where:
$\mathbf{x_{tc}}$ – feature vector for the tactile data.

Having the output of the transducer with 6 channels the dimensionality of the feature vector is 24. In Fig. 6 the calculated statistical values for F_z and T_x components of the signal are shown. The plot shows the variance, skewness and kurtosis calculated for the data gathered while walking on six different ground types (42 steps).

Additionally, feature vector was extended by calculating Fast Fourier Transform (FFT) of acquired signals. The plot of the FFT for F_z signal is shown in Fig. 7. As it could be observed, the highest response was obtained for the lowest frequency. This sample was excluded from the feature vector. It allows to avoid the problem of lowering the importance of the responses for subsequent frequencies in the classification process. The final vector was formed using 24 samples for each signal. After the 25th sample the responses are negligible. The feature vector consists of 24 responses for 6 channels which results in feature vector length equal to 144 dimensions.

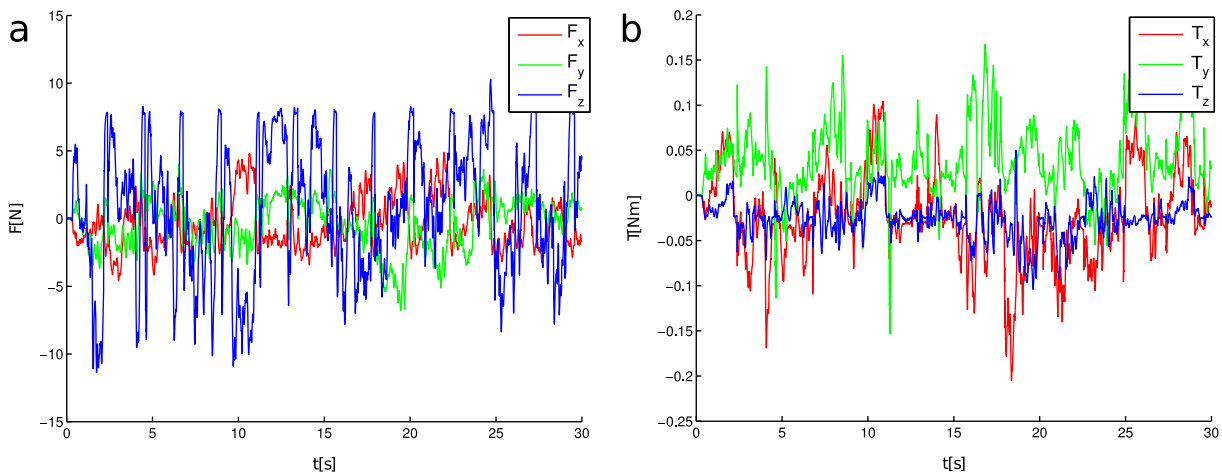

Fig. 5 Registered data from F/T sensor – robot walking on rocks: force signals **a**, torque signals **b**

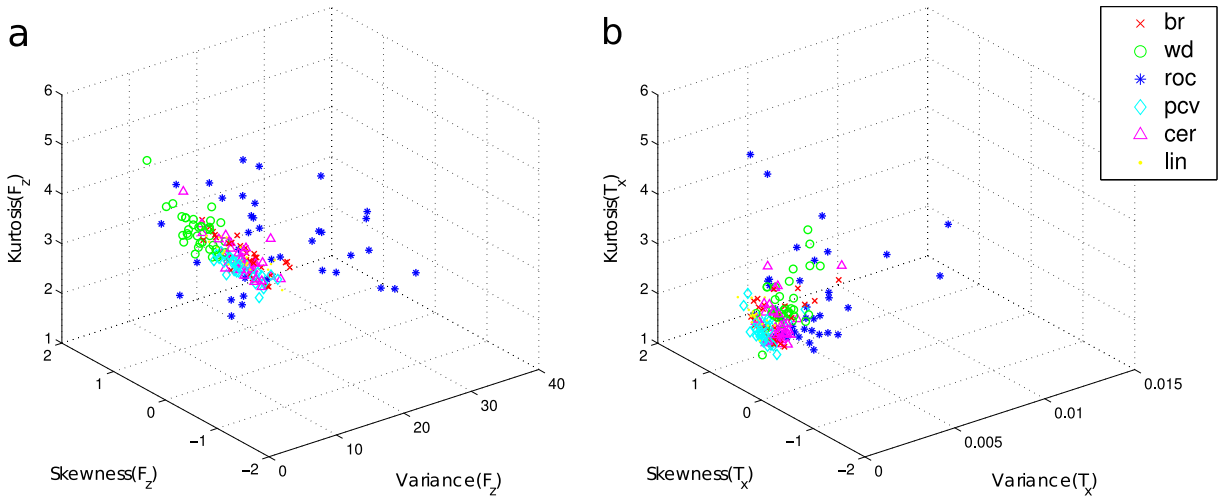

Fig. 6 Statistics computed from F/T signals for force **a** and torque **b** while walking on different types of the terrain. The ground types are: black rubber tiles(br), wooden boards(wd), rocks(roc), PVC tiles(pcv), ceramic tiles(cer) and carpet tiles(lin)

Results For the classification purposes the gathered data was divided into two sets: training – 30 steps, testing – 12 steps. The classifier was taught to identify 12 classes of the terrain. The training procedure was performed similarly to the one used for the point clouds. The result (precision) for the training set using statistical moments is equal to 80.83 % and for the testing set is equal to 76.39 %. The performance of the classifier, presented in the form of the confusion matrix, is shown in Fig. 8. The result (precision) for the training set using Fourier Transform is equal to 96.40 % and for the testing set is equal to 86.11 %. The performance of the classifier, presented in the form of the confusion matrix, is shown in Fig. 9. For the longer feature vector, which combines the statistical moments and Fourier transform, the results were the

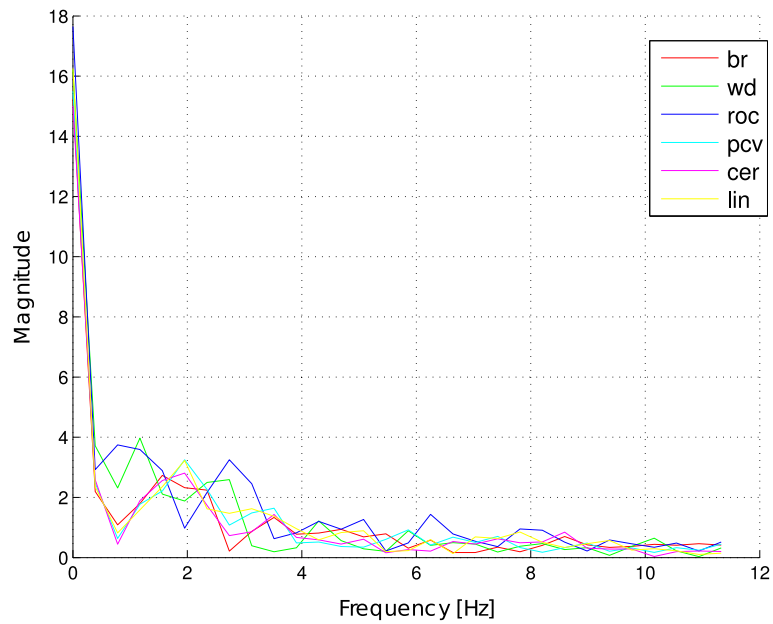

Fig. 7 Fast Fourier Transform of F_z signal – walking on different types of the ground. The ground types are: black rubber tiles(br), wooden boards(wd), rocks(stn), PVC tiles(pcv), ceramic tiles(cer) and carpet tiles(lin)

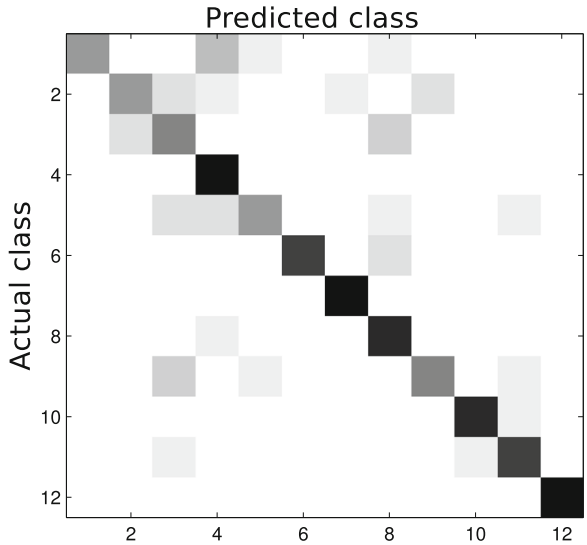

Fig. 8 Confusion matrix for classification of 12 terrain types using tactile perception – statistical moments. Classes names are: artificial grass(1), grit(2), pebbles(3), sand(4), green rubber tiles(5), concrete ground(6), black rubber tiles(7), wooden boards(8), rocks(9), PVC tiles(10), ceramic tiles(11) and carpet tiles(12)

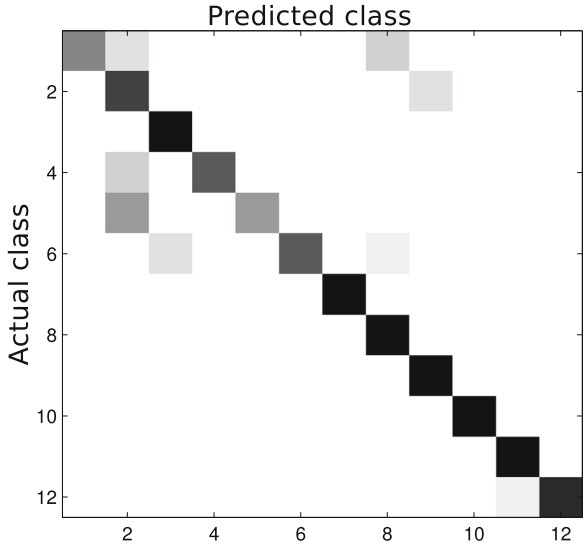

Fig. 9 Confusion matrix for classification of 12 terrain types using tactile perception – Fourier Transform. Classes names as in Fig. 8

same as for the Fourier data alone. The comparison of the obtained results for each classifier are shown in Table 1.

3.3 Visual Perception

The most popular approach to the terrain classification is the use of the RGB data. The suitability of the visual cues for the classification of our testing set with different terrain types was tested.

Data Acquisition The visual data was acquired using the RGB camera of the Kinect. The same points as in the part of the research regarding depth data were selected for the classification purposes using visual cues. The data was retrieved for different lighting conditions – daylight and artificial light (luminescent).

Features To obtain the feature vector, the approach similar to the one presented in [36] was adopted. The images were converted to the HSV colour space. Then, the mean and variance of hue and saturation of each patch was computed. Additionally, the histograms (10 bins) of hue and saturation for the patch were obtained.

$$\mathbf{x_{vs}} = [mean(H), var(H), mean(S), var(S), hist_{10}(H), hist_{10}(S)] \quad (3)$$

where:
$\mathbf{x_{vs}}$ – feature vector for the vision data;

The feature vector for each patch has 24 dimensions.

Results Similarly to the two earlier classification experiments SVM classifier was trained to identify 12 classes of the terrain. There were 84 sample patches for each type of the terrain. The training set consists of 60 samples and the testing set comprise 24 samples. The obtained overall precision for training set is equal to 90.41 %. However, for the testing set the performance is worse and the overall precision is equal to 69.79 %. The detailed performance of the classifier for the testing set, presented in the form of the confusion matrix, is shown in Fig. 10.

Table 1 Classification results for different classifiers

	Force stat.	Force Fourier	F stat and Fourier	Depth	Vision
Precision	0.7639	0.8611	0.8611	0.4792	0.6597
Recall	0.7970	0.9053	0.9070	0.4590	0.6011

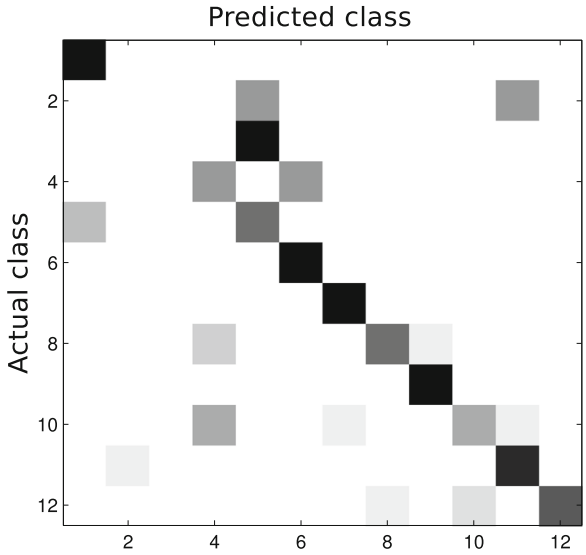

Fig. 10 Confusion matrix for classification of 12 terrain types using visual perception. Classes names are: artificial grass(1), grit(2), pebbles(3), sand(4), green rubber tiles(5), concrete ground(6), black rubber tiles(7), wooden boards(8), rocks(9), PVC tiles(10), ceramic tiles(11) and carpet tiles(12)

4 Combining Classifiers

In presented so far classification experiments, three types of the perception systems were used separately. Namely, depth, vision and tactile perception were tested. Having the results from several classifiers its is possible to merge them, to obtain better classification results. The weaknesses of one sensing modality could be complemented by the use of the different one. The SVMLIB, which was used to perform classification procedure, provides multi-class probability estimates for each testing sample. This property is required to perform combinations of the classfiers. When combining classifiers for each of the 12 terrain types, 12 testing samples of data, obtained for each sensing modality, were taken. The testing set for RGB and depth data is smaller comparing to one used in the experiments in the previous sections. The tactile perception set has cardinality equal to 12 for each terrain sample, so the cardinalities of the remaining sets were lowered. This allows to obtain equal cardinality of all three testing sets. The results of the classification for the smaller number of samples for each modality are shown in Table 1.

4.1 Combination Rules

According to [25] the responses of separate classifiers were combined, to obtain:

$$\text{assign } Z \rightarrow \omega \; if \; P(\omega_j|\mathbf{x}_1,\ldots,\mathbf{x}_R) = \max_k P(\omega_k|\mathbf{x}_1,\ldots,\mathbf{x}_R) \quad (4)$$

where:
$\mathbf{x_i}$ – measurements,
$i = 1 \ldots R$, where R is the number of classifiers;
Z – pattern;
$\omega_\mathbf{j}$ – class.

In our research four rules of combining classifiers were tested [25]:
Max rule:

$$\text{assign } Z \rightarrow \omega \; if \; \max_{i=1}^{R} P(\omega_j|\mathbf{x}_i) = \max_{k=1}^{m} \max_{i=1}^{R} P(\omega_k|\mathbf{x}_i) \quad (5)$$

Min rule:

$$\text{assign } Z \rightarrow \omega \; if \; \max_{i=1}^{R} P(\omega_j|\mathbf{x}_i) = \max_{k=1}^{m} \min_{i=1}^{R} P(\omega_k|\mathbf{x}_i) \quad (6)$$

Median rule:

$$\text{assign } Z \rightarrow \omega \; if \; \max_{i=1}^{R} P(\omega_j|\mathbf{x}_i) = \max_{k=1}^{m} \operatorname*{median}_{i=1}^{R} P(\omega_k|\mathbf{x}_i) \quad (7)$$

Product rule:

$$\text{assign } Z \rightarrow \omega \; if \; \max_{i=1}^{R} P(\omega_j|\mathbf{x}_i) = \max_{k=1}^{m} \prod_{i=1}^{R} P(\omega_k|\mathbf{x}_i) \quad (8)$$

The classification results, while using these four methods of combining classifiers for three different modalities, are shown in Table 2 – best results are marked using bold typeface. The result of the best classification strategy (product), in the form of the confusion matrix, is shown in Fig. 12.

Table 2 Classification results for combination of force (Fourier), depth and vision information

	min	max	median	prod
Precision	0.8681	0.8750	0.9236	0.9444
Recall	0.8956	0.8874	0.9298	0.9515

4.2 Influence of Different Sensing Modalities on Classification

Furthermore, the share of each modality in supporting base classifier (tactile) was checked. The results are shown in Table 3. It is clearly visible that, the use of the combined tactile and vision information about the terrain, gives the improvement by 5 % over the results obtained with the tactile information only. Further improvement was obtained by using depth data and it was equal to 2 %.

The results of combining only vision data with depth data and using different merging rules are shown in Table 4. Here the best performance was achieved for min rule. The confusion matrix for this case is shown in Fig. 11.

4.3 Data Acquisition Scenario

The results obtained for the combination of the different sensing modalities provide an opportunity to introduce the data acquisition scheme. When working in the real world conditions the scenario of gathering the knowledge about the environment, proposed in our earlier work [41], is as follows. The robot approaches the new terrain. From the distance the information about the terrain could only be gathered by using vision and depth sensors. The results of the classification using these two modalities are shown in Table 4 and in Fig. 11. The highest possible precision (min rule) is 79.86 % and recall 83.22 %. This is the certainty of the ground model which robot is able to achieve when standing in some distance from the new terrain. However, when the robot gets closer to the terrain and performs the first step on it the tactile information could be acquired. The confidence about the terrain class rises. The precision is now equal to 94.44 % and recall is equal to 95.15 %. While the robot moves towards the new terrain the confusion matrix shown in Fig. 11 transforms into confusion matrix shown in Fig. 12. Now the level of the robot confidence about the world model is sufficient to perform the control actions based on this type of a feed-back.

Table 3 Classification results for combination of force (Fourier) with depth or vision information

	Force Fourier and Depth	Force Fourier and Vision	Force and Vision and Depth
Precision	0.8611	0.9167	0.9444
Recall	0.8770	0.9298	0.9515

Table 4 Classification results for combination of depth and vision information

	min	max	median	prod
Precision	0.7986	0.6875	0.7014	0.7847
Recall	0.8322	0.6898	0.7071	0.8067

5 Controller

The information about the environment obtained by the perception system could be used for adjusting gait parameters of the walking robot to improve its motion capabilities. The walking process can generally be

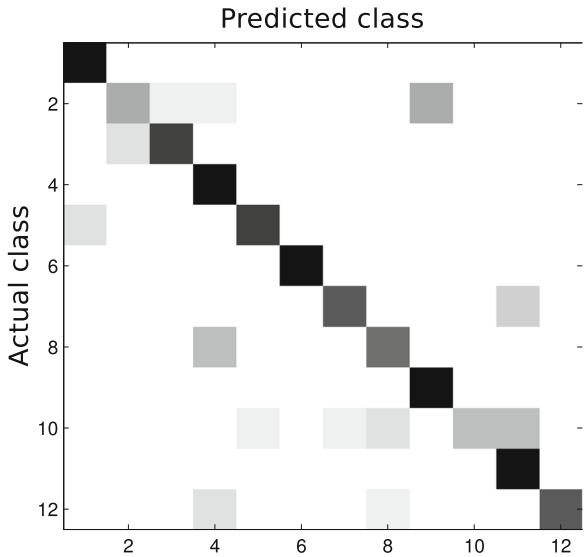

Fig. 11 Confusion matrix for classification of 12 terrain types using combination of depth and vision data by min rule. Classes names are: artificial grass(1), grit(2), pebbles(3), sand(4), green rubber tiles(5), concrete ground(6), black rubber tiles(7), wooden boards(8), rocks(9), PVC tiles(10), ceramic tiles(11) and carpet tiles(12)

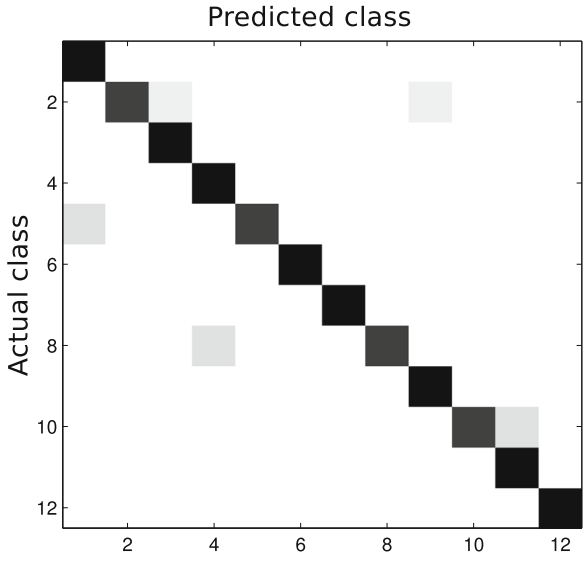

Fig. 12 Confusion matrix for classification of 12 terrain types using combination of tactile, depth and vision data by product rule. Classes names are: artificial grass(1), grit(2), pebbles(3), sand(4), green rubber tiles(5), concrete ground(6), black rubber tiles(7), wooden boards(8), rocks(9), PVC tiles(10), ceramic tiles(11) and carpet tiles(12)

divided into two phases: movement of a single leg, and the movement of the whole body of the robot.

Focusing on the movement of a single leg. The situation is shown in Fig. 13. It was assumed that the leg is in the appropriate position to start the leg cycle. In the first phase the leg is lifted – Fig. 13a. This phase is marked with the number (1). In the second phase the leg is moving freely in the direction of the indicated movement – Fig. 13b. This is the protraction phase and it is marked with the number (2). In the third phase the leg is lowered and placed on the ground – Fig. 13c. This is marked with the number (3). These three phases apply to a single leg.

The last phase is related to the movement of the whole body of the robot. In the three previous phases the leg was moving freely, but when the leg is kept on the ground, its movement causes the movement of the robot and has influence on the rest of the legs – Fig. 13d. This is the retraction phase marked with the number (4). In this phase the whole mass of the robot is moved forward (in this specific case) and is supported by all the legs of the robot.

Adjusting the parameters of each phase of the robot movement allows for more efficient negotiation of the diverse terrains. In our research we are using a six-legged walking robot equipped with position controlled servomotors. The robot is using Hitec

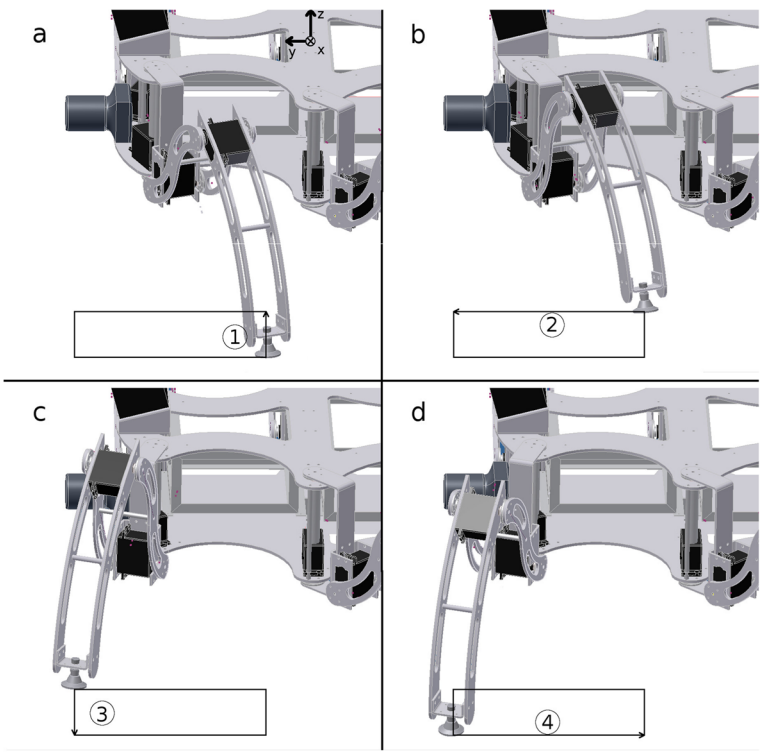

Fig. 13 Phases of the leg movement: **a** – lift the leg (1), **b** – move the leg (2), **c** – lower the leg (3), **d** – move the body of the robot (4)

HSR-5990TG with HMI (Hitec Multi-protocol Interface) which allows only to change P and D gain of the internal controller using three fixed values. Therefore, the only possible modification of the gait parameters is the change of the speed of the leg movement in each phase of the walk.

To asses the performance of the robot while walking on different terrains, the measurements of the acceleration of the robot body were performed. According to [31], due to the change of the mechanical properties of the terrain, robot's legs provide different push based on the ground type they are interacting with. Therefore, the vertical acceleration of the robot is an informative feature.

5.1 Performed Experiments

In order to develop control law for the robot the series of experiments were performed. Namely, the robot was walking on 12 terrain types with different settings of the speed parameters for each phase of the gait. During each trial the vibration on the robot chassis were measured using a 3-axis accelerometer, which is a part of the AHRS – Xsens MT-28A53G25. The sensor provides the calibrated readings of the accelerations of the robot along each axis of the local coordinate frame. The local coordinates frame of the robot is shown in Fig. 13a. In each trial robot was performing 3 complete gait cycles using a wave gait. This gives 18 steps for each trial. The grid search of the gait parameters was performed. Two speeds for lifting the leg, phase (1), were selected. Namely 0.5 and 0.8 of maximum servomotor speed, which is in our case 2.38 rad/s. The speed parameter of putting the leg down $V_{leg_{down}}$, phase (3), had 7 possible values. The range of speeds for $V_{leg_{down}}$ was [0.2, 0.8] with the iteration step equal to 0.1 of maximum servomotor speed. The speed of the movement for the phase (2) and (4) are set to 0.8 of maximum servomotor speed. The robot should move as fast as possible. The mean values of the acceleration measured, along axes x, y and z, during the experiments are shown in Figs. 14, 15 and 16 respectively.

In order to compensate the biases of the acceleration readings the AHRS was placed on the floor of the laboratory and the measurements were taken for 52 sec and the mean values of the accelerations along each axis of the local coordinates

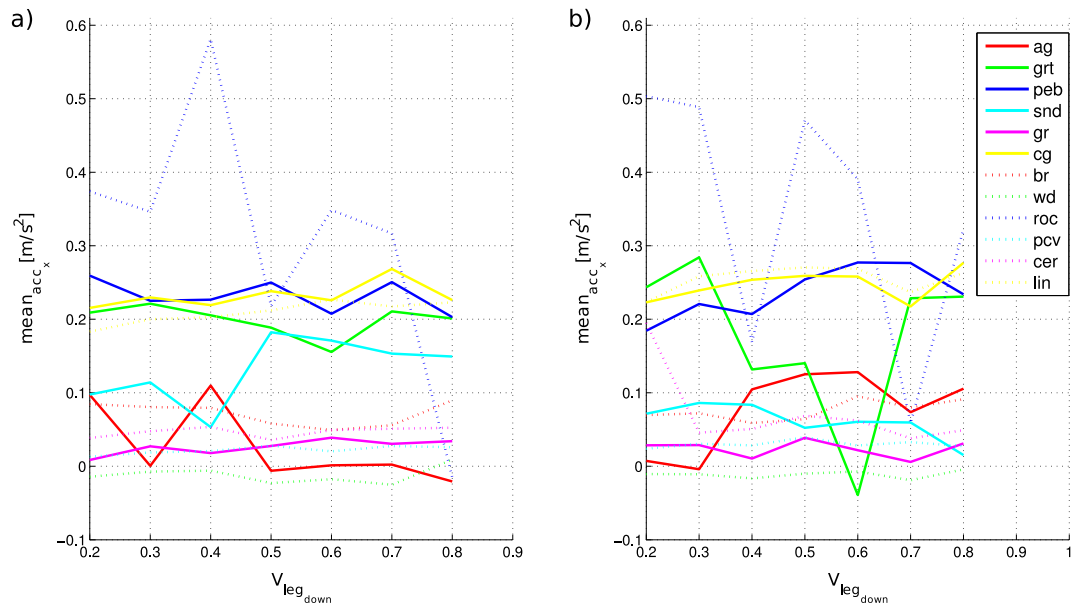

Fig. 14 Mean value of acceleration along x-axis of the robot while changing the speed of lowering the leg. Experiments performed for two lifting speeds a) 0.5 b) 0.8 maximum speed of the motor and 12 terrain types. Classes names are: artificial grass(ag), grit(grt), pebbles(peb), sand(snd), green rubber tiles(gr), concrete ground(cg), black rubber tiles(br), wooden boards(wd), rocks(roc), PVC tiles(pcv), ceramic tiles(cer) and carpet tiles(lin). $V_{leg_{down}}$ – fraction of the maximum motor speed

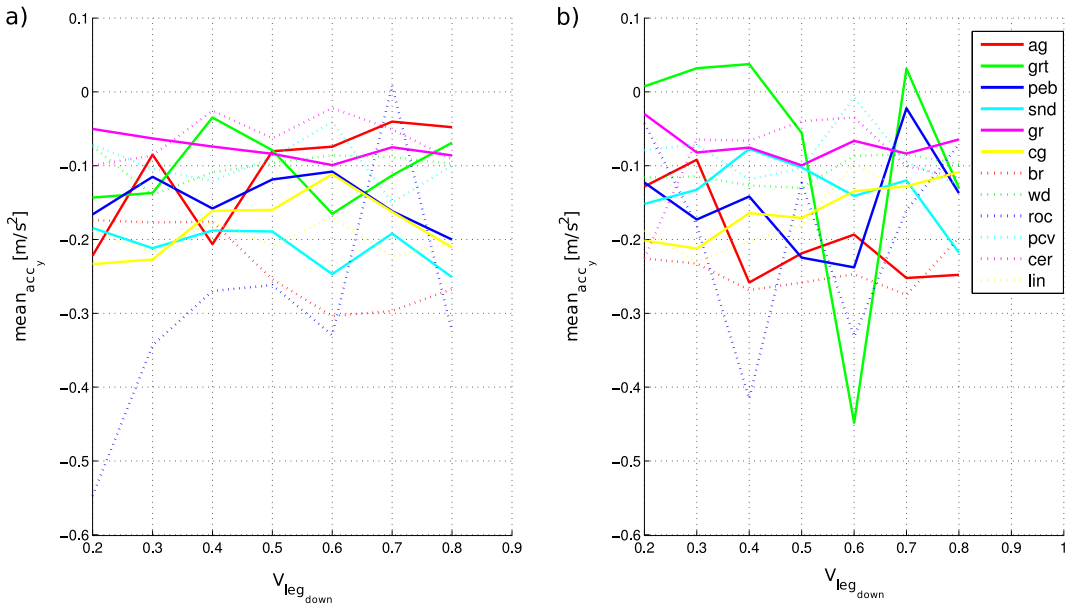

Fig. 15 Mean value of acceleration along y-axis of the robot while changing the speed of lowering the leg. Experiments performed for two lifting speeds a) 0.5 b) 0.8 maximum speed of the motor and 12 terrain types. Classes names as in Fig. 14. $V_{leg_{down}}$ – fraction of the maximum motor speed

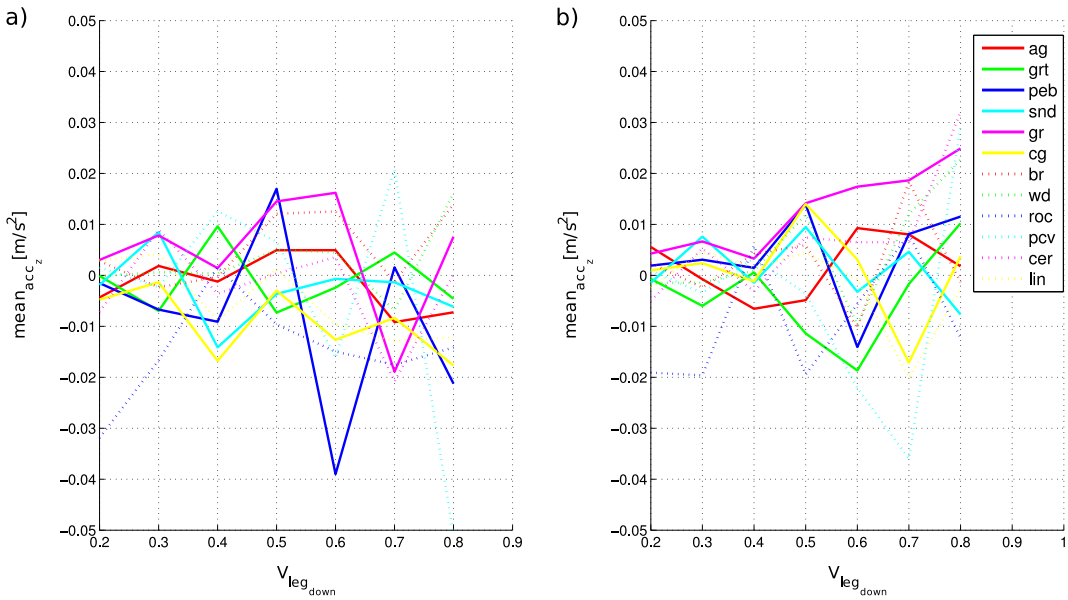

Fig. 16 Mean value of acceleration along z-axis of the robot while changing the speed of lowering the leg. Experiments performed for two lifting speeds **a** 0.5 **b** 0.8 maximum speed of the motor and 12 terrain types. Classes names as in Fig. 14. $V_{leg_{down}}$ – fraction of the maximum motor speed

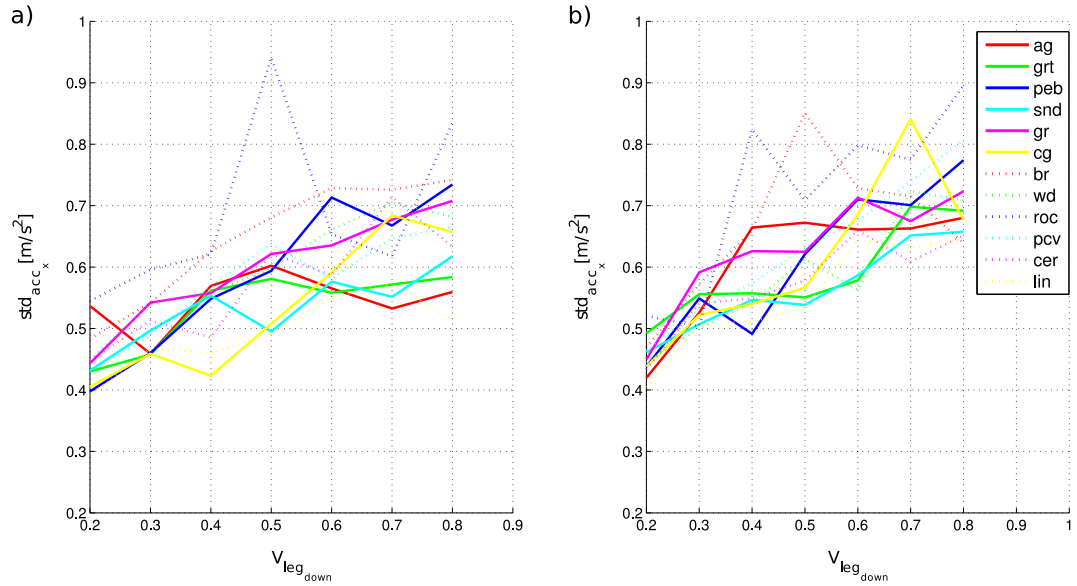

Fig. 17 Standard deviation of acceleration along x-axis of the robot while changing the speed of lowering the leg. Experiments performed for two lifting speeds **a** 0.5 **b** 0.8 maximum speed of the motor and 12 terrain types. Classes names are: artificial grass(ag), grit(grt), pebbles(peb), sand(snd), green rubber tiles(gr), concrete ground(cg), black rubber tiles(br), wooden boards(wd), rocks(roc), PVC tiles(pcv), ceramic tiles(cer) and carpet tiles(lin). $V_{leg_{down}}$ – fraction of the maximum motor speed

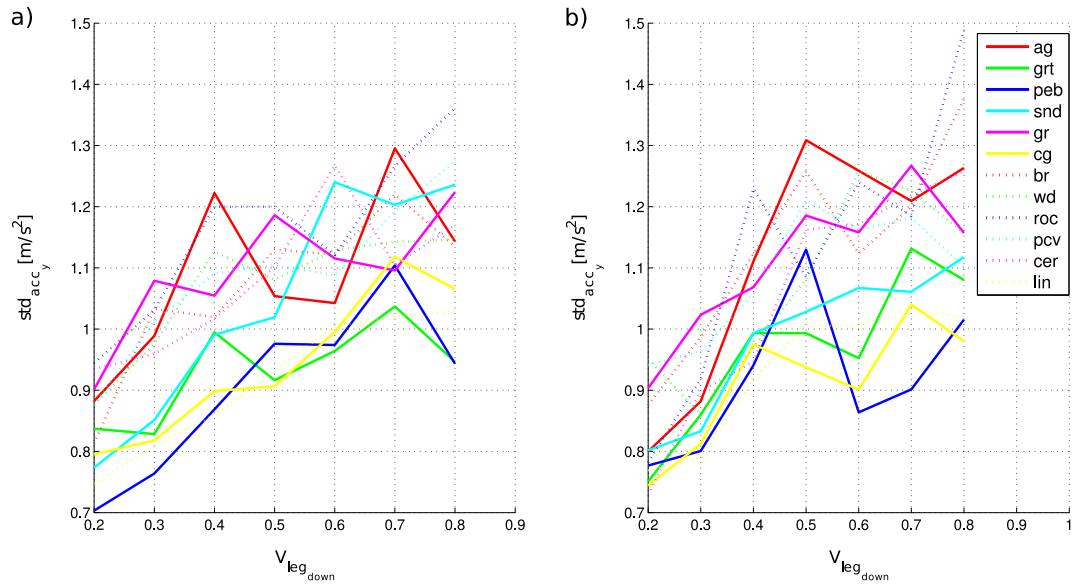

Fig. 18 Standard deviation of acceleration along y-axis of the robot while changing the speed of lowering the leg. Experiments performed for two lifting speeds **a** 0.5 **b** 0.8 maximum speed of the motor and 12 terrain types. Classes names as in Fig. 17. $V_{leg_{down}}$ – fraction of the maximum motor speed

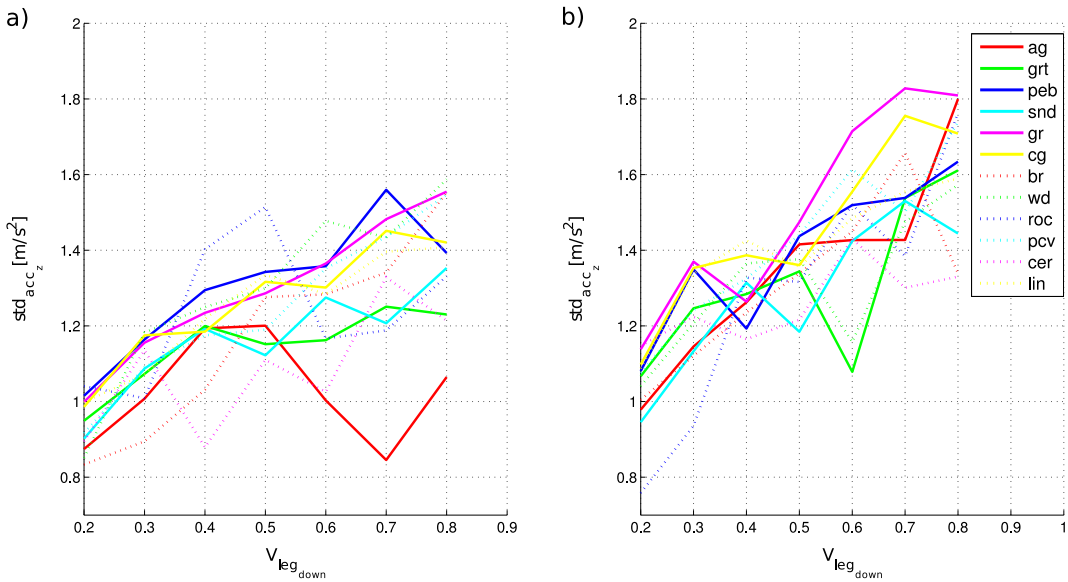

Fig. 19 Standard deviation of acceleration along z-axis of the robot while changing the speed of lowering the leg.Experiments performed for two lifting speeds **a** 0.5 **b** 0.8 maximum speed of the motor and 12 terrain types. Classes names as in Fig. 17. $V_{leg_{down}}$ – fraction of the maximum motor speed

frame of the AHRS were computed. The values of the biases for the sensor were equal to $a_b = [0.0616, 0.0303, 9.8217]\ m/s^2$. The third value of the vector is the gravitational acceleration measured with oursensor.

As it could be observed, the terrain type has the influence on the acceleration of the robot body while walking. For the dry sand, which is absorbing most of the foot bounce, the acceleration values in z-axis are not changing noticeably while changing the speed of putting the leg down. On the contrary, noticeable bounce of the robot could be observed when walking on the stiff surfaces such as concrete floor.

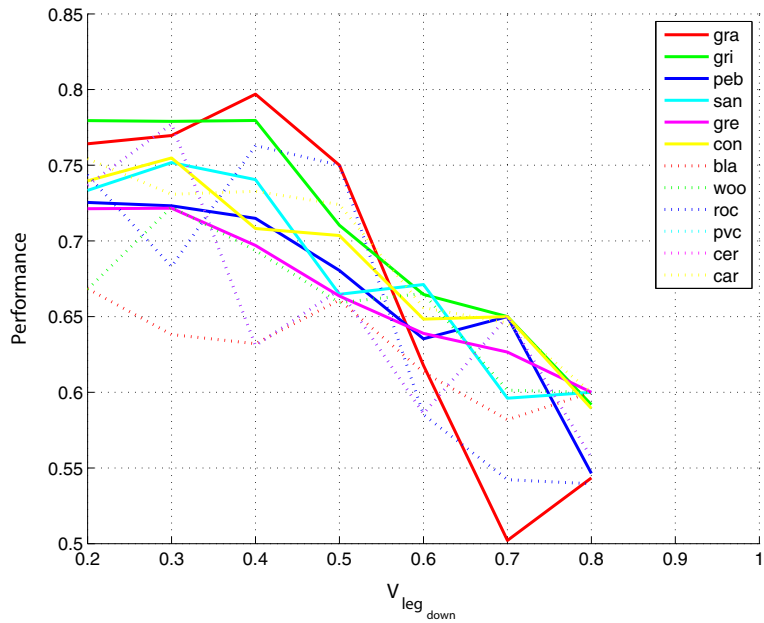

Fig. 20 Plot of the performance function for lifting speed 0.5 of maximum speed of the motor and 12 terrain. Classes names are: artificial grass(ag), grit(grt), pebbles(peb), sand(snd), green rubber tiles(gr), concrete ground(cg), black rubber tiles(br), wooden boards(wd), rocks(roc), PVC tiles(pcv), ceramic tiles(cer) and carpet tiles(lin). $V_{leg_{down}}$ – fraction of the maximum motor speed

However, to obtain better understanding of the relation between the terrain type and the speed of lowering the leg, standard deviation of the acquired signals were calculated. The standard deviations of the accelerations along axes x, y, z are shown in Figs. 17, 18 and 19 respectively.

The standard deviation provides the overview of the range in which the acceleration is changing. For the x-axis the values of the standard deviation are not exceeding 0.95 m/s^2 and for the y-axis the maximum value is equal to 1.5 m/s^2. For the z-axis the value of standard deviation is exceeding 1.8 m/s^2. The accelerations of the robot along the x-axis and y-axis are caused by the forward movement of the robot. Whereas, the acceleration in z-axis is mostly influenced by the terrain characteristics. The higher the standard deviation of the acceleration, the more bumpy terrain is. Therefore, while walking, more energy is dissipated for the unnecessary lifting of the robot chassis. Hence, the acceleration along z-axis should be considered as a feedback signal for the gait controller.

5.2 Controller Synthesis

Having the data obtained in the grid search procedure, the control law was proposed. The robot is required to move as fast as possible while retaining the small vibrations. Thus, it is not loosing to much of its energy on other movements then those required for the forward displacement. Looking at the figures the most energy is lost for the movements along z-axis (up and down). Hence, our control law is based on the standard deviation of the accelerations along the z-axis weighted by the $V_{leg_{down}}$. The penalty is assigned for the slower speed of the forward movement $(1 - V_{leg_{down}})$. The control law is given by equation:

$$Performance = min[(1 - V_{leg_{down}} + Std_{z_{norm}})/2] \tag{9}$$

where:
$V_{leg_{down}}$ – speed of putting leg down, fraction of the maximum motor speed [0;1];
$Std_{z_{norm}}$ – normalized standard deviation of acceleration along z-axis [0;1];

Both components have values from [0;1] hence by dividing the obtained value by 2 the $Performance$ is also from range [0;1].

The results of searching the minimum from 9, for the leg lifting speed equal to 0.5, gait phase (2), are shown in Fig. 20. The minimum for each class is more visible in the bar graph (Fig. 21). As it could be observed, the whole set is divided into two groups. These terrains which could be negotiated efficiently with 0.8 of the maximum speed and those which could be traversed with speed 0.7. Using our control law for the speed of lifting the leg equal to 0.8 three groups of the terrain were identified. Those which are negotiated efficiently with 0.8, 0.7 and 0.6 of the maximum servomotor speed. This could be observed in Fig. 22 and also in the bar graph in Fig. 23. The obtained results allows for proposing a discrete controller.

5.3 Controller Implementation

The specification of the controller was established by using the Discrete Event Systems approach. The definition of the deterministic automaton is stated according to [12]. Supervisor S is defined as:

$$S_{vc} = (X_{vc}, E_{vc}, f_{vc}, x_{vc0}, X_{vcm}), \tag{10}$$

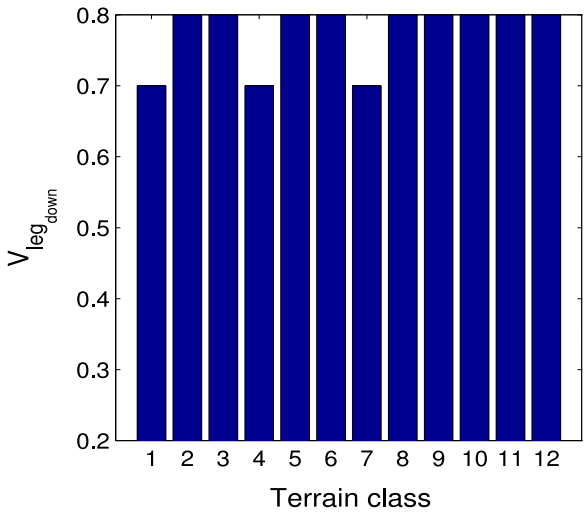

Fig. 21 $V_{leg_{down}}$ minimum for each terrain for lifting speed 0.5 of maximum speed of the motor and 12 terrain types. Classes names are: artificial grass(1), grit(2), pebbles(3), sand(4), green rubber tiles(5), concrete ground(6), black rubber tiles(7), wooden boards(8), rocks(9), PVC tiles(10), ceramic tiles(11) and carpet tiles(12). $V_{leg_{down}}$ – fraction of the maximum motor speed

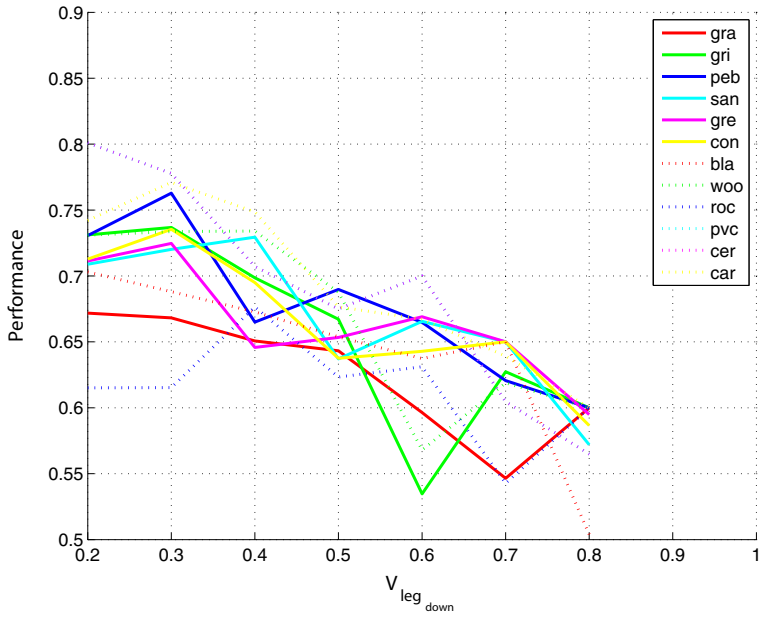

Fig. 22 Plot of the performance function for lifting speed 0.8 of maximum speed of the motor and 12 terrain. Classes names as in Fig. 20. $V_{leg_{down}}$ – fraction of the maximum motor speed

where:

X_{vc} is the set of *states allowed in the specification* of the velocity controller,

E_{vc} is the finite set of *events associated with* S_{vc},

$f_{vc} : X_{vc} \times E_{vc} \rightarrow X_{vc}$ is the *transition function,*

x_{vc0} is the *initial state,*

$X_{vcm} \subseteq X_{vc}$ is the set of *marked states.*

The automaton consists of 3 states:

$$X_{vc} = \{V_{08}, V_{07}, V_{06}\}, \tag{11}$$

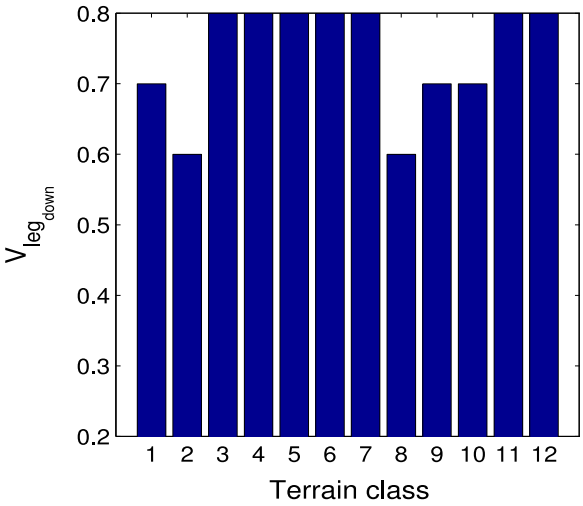

Fig. 23 $V_{leg_{down}}$ minimum for each terrain for lifting speed 0.8 of maximum speed of the motor and 12 terrain types. Classes names are as in Fig. 21

where:

V_{0n} : encodes the speed of the down movement of the leg – phase (3) of the gait,

n = 6,7,8.

Transitions from state to state are driven by events. The number of events is 6, as it was defined in (12).

$$E_{vc} = ag, roc, pcv, grt, wd, nt. \tag{12}$$

where:

ag : artificial grass,

roc : rocks,

pcv : PVC tiles,

grt : grit,

wd : wooden boards,

nt : neutral;

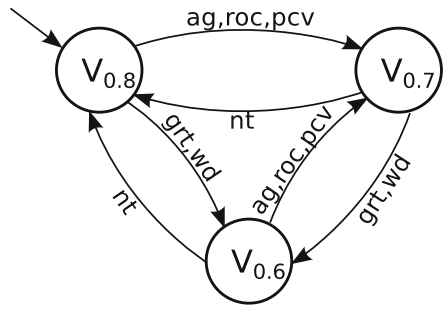

Fig. 24 Control strategy based on $V_{leg_{down}}$ for lifting speed 0.8

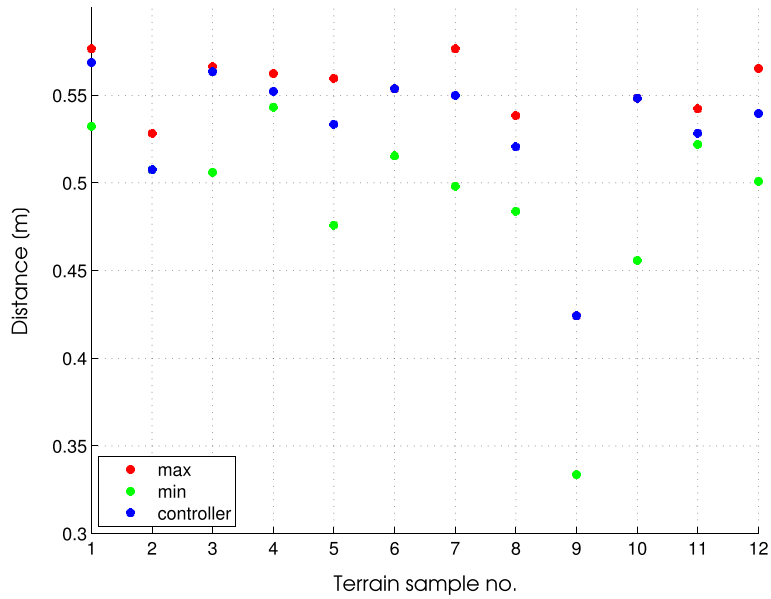

Fig. 25 Controller evaluation (distance travelled) for lifting speed 0.8 of maximum speed of the motor and 12 terrain types. Classes names are: artificial grass(1), grit(2), pebbles(3), sand(4), green rubber tiles(5), concrete ground(6), black rubber tiles(7), wooden boards(8), rocks(9), PVC tiles(10), ceramic tiles(11) and carpet tiles(12). Red dots – best result, green dots – worst result; blue dots – controller

In the synthesis of the controller the signals from the perception system were assumed to be deterministic due to high precision and recall of the obtained classifier. The controller is shown in Fig. 24.

5.4 Controller Evaluation

For the proposed controller, evaluation procedure was performed. The experimental setup consisted of a camera mounted on the robot and a chessboard mounted on the pole standing in front of the robot. The camera was calibrated beforehand using calibration toolbox [5]. Next, the distance estimation error was checked. To achieve this goal CNC (Computer Numerical Control) milling-machine with the precise measurement of the feed (0.001 mm) was used as the moving table. For the distance of 1.2 m from the camera to the chessboard the average error of distance

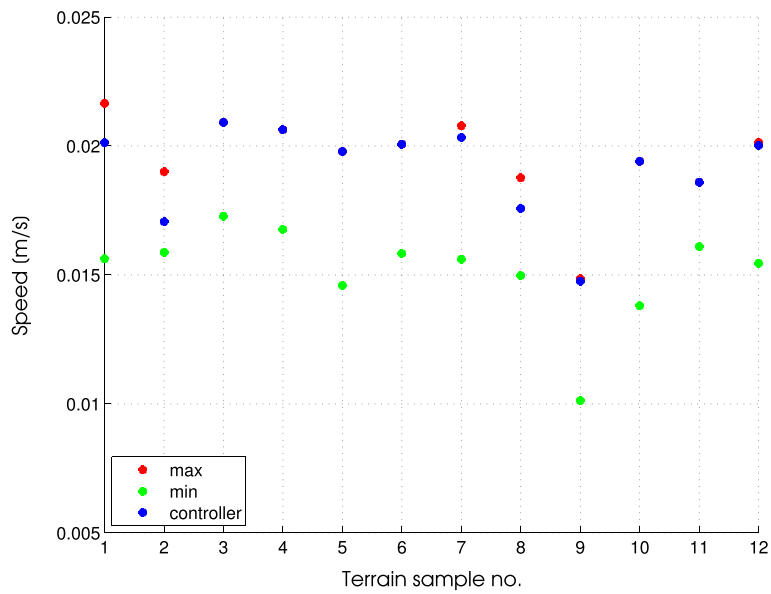

Fig. 26 Controller evaluation (speed of the robot) for lifting speed 0.8 of maximum speed of the motor and 12 terrain types. Classes names are as in Fig. 25. Red dots – best result, green dots – worst result; blue dots – controller

measurements (20 trials 0.5 mm feed each) was equal to 0.57 mm with standard deviation of 0.37 mm.

With the properly calibrated camera, robot was performing trials of 8 steps, of the same length, going forward on each terrain type. Leg lifting speed was set to 0.8 and leg lowering speed was adjusted from 0.5 – 0.8. The distance travelled by the robot for the best and worst trials is shown in Fig. 25 using red and green dots respectively.

While measuring the distance proper measurements of time were performed as well. Each grabbed frame was timestamped. Using this information the speed of the robot movement for each trial was calculated. The speed of the robot movement for the best and worst trials is shown in Fig. 26 using red and green dots respectively.

The qualitative controller evaluation for the travelled distance is shown in Table 5. As it could be observed, the proposed controller is sub-optimal. In several cases better results were measured. In the worst case the maximum difference in the travelled distance between the robot using proposed controller and the best result achieved is equal to 0.0265 m. Relating this to the maximum difference between the best and worst value measured during the experiments, which is 0.0927 m, the gain of using the proposed controller is clearly visible. Describing the results statistically, mean difference between the controller and optimal solution is equal to 0.0126 m with standard deviation of 0.0106 m. Whereas, comparing optimal solution with worst results, average difference is equal to 0.0555 m with standard deviation of 0.0273 m.

The qualitative controller evaluation for the speed of robot forward movement is shown in Table 6. Using speed as the controller performance measure, the obtained results indicate even closer performance resemblance of the proposed controller to the optimal solution. In the worst case the maximum difference in the movement speed between the robot using proposed controller and the optimal trial is equal to 0.0019 m/s comparing to worst value achieved which is 0.0060 m/s. Describing the results statistically mean difference between the controller and optimal solution is equal to 0.0004 m/s with standard deviation of 0.0007 m/s. Whereas, comparing optimal solution with worst results, average difference is equal to 0.0044 m/s with standard deviation of 0.0010 m/s.

In 9 cases out of 12 the proposed controller is matching the best results achieved when measuring speed of the robot movement on different terrain types.

Table 5 Controller evaluation – travelled distance

	$min[m]$	$max[m]$	$\mu[m]$	$\sigma[m]$
best-worst	0.0191	0.0927	0.0555	0.0273
best-controll.	0.0000	0.0265	0.0126	0.0106

Table 6 Controller evaluation – speed of movement

	$min[m/s]$	$max[m/s]$	$\mu[m/s]$	$\sigma[m/s]$
best-worst	0.0025	0.0060	0.0044	0.0010
best-controll.	0.0000	0.0019	0.0004	0.0007

6 Discussion

In this section the comparison of the obtained results with other similar approaches is given. The qualitative and quantitative comparison will be made. For the terrain classification it is possible to give the exact numbers and compare the results quantitatively. However, it is hard to differentiate the controllers of the walking robots due to the fact that the experiments described in each of the papers are performed on different machines. A common testing platform is not available at the moment.

6.1 Quantitative Comparison

The results regarding terrain classification which were presented in the current paper were compared against eight other approaches. This is shown in Table 7. In this table not only bare classification results, but also the type of the sensor used and the number of terrain classes recognized by the classifier were presented. Our approach has similar results (precision) to the results obtained in the work reported in [13] and in [17]. However, in [13] the dataset is two times smaller. In the second case, even though the cardinality of the datasets is comparable, the experiments were performed in the controlled manner. The speed of the wheeled robot movement was constant for each experimental trial. This is not possible in the case

Table 7 Comparison of the results with other approaches

	No. of terrain classes	Results (precision)	Sensors used	Notes
Bermudez [4]	3	93.80 %	IMU, back-EMF, magnetic encoders	
Manjanna [31]	4	92.11 %	IMU, motor current	
Filitchkin [13]	6	95.40 %	Vision	interclass variability
Angelova [1]	7	78.85 %	Vision	interclass variability
Zenker [50]	8	91.46 %	Vision	moving walking robot
Giguere [17]	10	94.60 %	Tactile probe	
Hoepflinger [19]	11	86.81 %	F/T sensor – single vibrating leg	no robot motion
Weiss [48]	14	87.33 %	Vision, Vibration	
Our approach	12	94.44 %	F/T sensor, depth, vision	

of the walking robot. For the slightly larger dataset described in [48], the results of the terrain classification using vision and vibration information were lower by 7 % comparing to the approach proposed in this paper.

When referring to the results reported in [19] it is worth noting that the results obtained for 11 terrains using tactile sensing (86.81 %) are similar to the one presented in this paper when utilizing only F/T sensor (86.11 %). Even though, their approach might seem similar to ours, but in fact there is a major difference. Their experiments were performed using single robotic leg removed from the robot. Additionally, there is no direct connection of the presented work with the control of the robot gait. Hence, this work will not be covered in the qualitative comparison.

6.2 Qualitative Comparison

The control system of the robot due to the lack of the common platform for testing could only be compared in the qualitative manner. The common platform is understood as the use of the same walking robot and the same ground samples.

The comparison starts from the work reported in [13]. The robotic platform, used in the experiments, was four legged Little Dog. The robot was traversing 5 terrain types. The classification results were employed for changing preprogrammed gait patterns. As a gait adjusting parameter ground clearance was chosen. Three gait types with: low, medium and high ground clearance were tested. The times of the terrain negotiation were measured while using each gait and then the classification results were used to select the appropriate gait for each terrain class.

Next, let us focus on paper [4] which describes experiments performed for a milirobotic crawling platform. The change of the speed of the robot movement on each terrain type was tested against the stride frequency. However, the classification results weren't directly implemented to control the robot.

In publication [50] terrains were divided into four different groups: stiff ground, loose ground, rough ground, vegetated ground and the experiments were performed while measuring energy consumption while walking on each terrain type. In the performed experiment, control input value of the Central Pattern Generator (CPG) was modified and tested.

Finally, in work reported in [18] the experiment, which was only the proof of the concept, the Rhex robot was able to identify three terrain types: beach, wash and water. Based on the classification results robot switched its control mode from gait to swimming. In this experiment the authors used only the threshold rule to classify the terrains. As more challenging experiment the classification of linoleum, snow and ice was performed. Obtained average precision was equal to 92.67 %, but no experiments with controller were performed. Recently the research was extended in [31]. In this research the tests on how the walking speed is influencing terrain identification process were performed.

In the approach presented in this paper Discrete Event Controller was built. The proposed controller

was obtained by optimising gait parameters using robot chassis vibration data. The preprogrammed gaits were not used. In this sense our approach is more advanced then these presented in above-mentioned comparison. Additionally, aforementioned approaches were adjusting the speed of the whole robot, where in approach presented in this paper the leg movement phases were treated separately in the controller synthesis process.

6.3 Limitations

In the presented approach several limitations could be noticed. Firstly, the depth perception experiments were performed for the terrain samples lying on the horizontal plane. No test with the inclined terrains were performed. It was assumed that the ground plane could be calculated from the point cloud and then it could be transformed to the appropriate reference frame. But looking at the nature of the measurements, the terrain seen from different angles could have totally different shape for example due to the occlusions.

Additionally, the depth sensor is providing information about the terrain geometry which is not always related to the terrain type. It is mostly observed for the loose terrains, where the geometry may change, for example, due to the robot movement. However, for several terrain types the geometry is fixed (e.g. ceramics, wooden boards) and the information about the geometry is the relevant feature to support features obtained from other sensing modalities.

In the controller part some limitations could also be found. The proposed control law is suitable for the terrain types presented in the paper. The set of samples is not covering the whole range of the terrain types. The most important fact is that the thorough test of the influence of changing friction coefficient (in the wide range) were not performed. For example, no results were obtained for the robot walking on ice or wet slippery surfaces. The research was focused mainly on the compliance and irregularities of the ground and how they influence the bounce of the robot foot.

7 Conclusions

In the presented paper the system for improving mobility of the walking robot in the changing terrain conditions was presented. The robot was equipped with three types of the perception systems to obtain the information about the ground class. The classification results for each of the perception systems used separately weren't satisfactory to obtain the reliable estimate of the ground type. However, the utilization of the classifier combination rules allowed to obtain the precision and recall results above 94 %. This level of the confidence allowed us to built the controller which relayed on the information from the perception system. The discrete controller which adjust the speed of the robot movements to the type of the terrain was proposed. The condition to be fulfilled is to obtain the balance between the speed of the forward displacement of the robot and in the same time to reduce the energy lose caused by the vibrations of the robot trunk while traversing different terrain types.

The obtained results of the terrain classification are comparable to the results obtained in the similar research. However, it is worth mentioning that in our case the similar percentage of good classifications was obtained for the larger dataset. Additionally, the proposed controller was obtained in the optimisation process and is not using the preprogrammed gaits. This indicates the progress which is made comparing to the previous approaches. The obtained controller was evaluated with the external system for distance and movement speed measurements.

The results obtained in the experiments described in this paper allows us to envision some future directions of the research on adaptation of the walking robot gait to the ground type. In the classification process the experiments with different directions of the robot movement and different walking speeds should be performed. This would enable the robot to perform challenging tasks in real world scenario such as Search and Rescue Missions.

Furthermore, the influence of the different optimisation functions, used in the process of the gait controller synthesis, on effectiveness of the terrain negotiation should be checked. Additionally, to check the whole variety of the control schemes, the walking robot should be equipped with torque controllable servomotors. It will enable us to exploit the knowledge from the field of robotic manipulators and make the robot legs fully compliant.

References

1. Angelova, A., Matthies, L., Helmick, D.M., Perona, P.: Fast te rrain classification using variable-length representation for autonomous navigation. In: CVPR. IEEE Computer Society (2007)
2. Bellone, M., Reina, G., Giannoccaro, N.I., Spedicato, L.: Unevenness point descriptor for terrain analysis in mobile robot applications. Int. J. Adv. Robot. Syst. **10**, 1–10 (2013)
3. Belter, D., Skrzypczynski, P.: Rough terrain mapping and classification for foothold selection in a walking robot. J. Field Robot **28**(4), 497–528 (2011)
4. Bermudez, F.G., Julian, R.C., Haldane, D.W., Abbeel, P., Fearing, R.S.: Performance analysis and terrain classification for a legged robot over rough terrain. In: IROS, pp. 513–519. IEEE (2012)
5. Bradski, G.: The openCV Library. Dr. Dobb's J. Softw. Tools **25**(11), 120–126 (2000)
6. Bretl, T.: Motion planning of multi-limbed robots subject to equilibrium constraints: the free-climbing robot problem. I. J. Robot. Res. **25**(4), 317–342 (2006)
7. Brooks, C., Iagnemma, K.: Vibration-based terrain classification for planetary exploration rovers. Robot. IEEE Trans. **21**(6), 1185–1191 (2005)
8. Brooks, R.: A robot that walks; emergent behaviors from a carefully evolved network. In: Proceedings of the IEEE International Conference on Robotics and Automation, 1989, vol. 2, pp. 692–4+2 (1989)
9. Buss, M., Schmidt, G.: Hybrid system behavior specification for multiple robotic mechanisms. In: IROS, pp. 140–147. IEEE (1996)
10. Chang, C.C., Lin, C.J.: LIBSVM: a library for support vector machines. ACM Trans. Intell. Syst. Tech. **2**, 27:1–27:27 (2011)
11. Chemori, A., Le Floch, S., Krut, S., Dombre, E.: A control architecture with stabilizer for 3D stable dynamic walking of SHERPA biped robot on compliant ground. In: 10th IEEE-RAS International Conference on Humanoid Robots (Humanoids), 2010, pp. 480–485 (2010)
12. Christos, C., Lafortune, S.: Introduction to Discrete Event Systems – second edition. Springer Science+Business Media, New York (2008)
13. Filitchkin, P., Byl, K.: Feature-based terrain classification for LittleDog. In: IROS, pp. 1387–1392. IEEE (2012)
14. Genya, I., Masatsugu, O., Takashi, K.: Lidar-based Terrain Mapping and Navigation for a Planetary Exploration Rover. In: Proceedings of the International Symposium on Artificial Intelligence, Robotics and Automation in Space (i-SAIRAS)'12 (2012)
15. Giguere, P., Dudek, G.: Clustering sensor data for autonomous terrain identification using time-dependency. Auton. Robot. **26**(2-3), 171–186 (2009)
16. Giguere, P., Dudek, G.: Surface identification using simple contact dynamics for mobile robots. In: ICRA'09 IEEE International Conference on Robotics and Automation, 2009, pp. 3301–3306 (2009)
17. Giguere, P., Dudek, G.: A simple tactile probe for surface identification by mobile robots. Robot. IEEE Trans. **27**(3), 534–544 (2011)
18. Giguère, P., Dudek, G., Saunderson, S., Prahacs, C.: Environment identification for a running robot using inertial and actuator cues. In: Sukhatme, G.S., Schaal, S., Burgard, W., Fox, D. (eds.) Robotics: Science and Systems. The MIT Press (2006)
19. Hoepflinger, M., Remy, C., Hutter, M., Haag, S., Siegwart, R.: Haptic Terrain Classification on Natural Terrains for Legged Robots. In: Proceedings of the 13th International Conference on Climbing and Walking Robots (CLAWAR), pp. 785–792, World Scientific (2010)
20. Hoepflinger, M., Remy, C., Hutter, M., Spinello, L., Siegwart, R.: Haptic terrain classification for legged robots. IEEE International Conference on Robotics and Automation (ICRA), 2010, pp. 2828–2833 (2010)
21. Howard, A.M., Parker, L.T.: A hierarchical strategy for learning of robot walking strategies in natural terrain environments. In: Proceedings of the ISIC. IEEE International Conference on System Management and Cybernetics (SMC 07), pp. 2336–2341 (2007)
22. Iagnemma, K., Dubowsky, S.: Mobile robots in rough terrain - estimation, motion planning, and control with application to planetary rovers. Springer Tracts in Advanced Robotics, vol. 12, Springer (2004)
23. Izumi, K., Sato, R., Watanabe, K.: Generation of obstacle avoidance behaviors for quadruped robots using finite automaton. In: SICE Annual Conference, 2008, pp. 2523–2527 (2008)
24. Kalakrishnan, M., Buchli, J., Pastor, P., Mistry, M., Schaal, S.: Fast, robust quadruped locomotion over challenging terrain. In: ICRA, pp. 2665–2670. IEEE (2010)
25. Kittler, J., Hatef, M., Duin, R.P.W., Matas, J.: On Combining Classifiers. IEEE Trans. Pattern Anal. Mach. Intell. **20**(3), 226–239 (1998)
26. Kroemer, O., Lampert, C., Peters, J.: Learning dynamic tactile sensing with robust vision-based training. Robot. IEEE Trans. **27**(3), 545–557 (2011)
27. Laible, S., Khan, Y., Bohlmann, K., Zell, A.: 3D LIDARand camera-based terrain classification under different lighting conditions. In: Levi, P., Zweigle, O., Häuβermann, K., Eckstein, B. (eds.) Autonomous Mobile Systems 2012, Informatik aktuell, pp. 21–29. Springer, Heidelberg (2012)
28. Lalonde, J.F., Vandapel, N., Huber, D., Hebert, M.: Natural terrain classification using three-dimensional ladar data for ground robot mobility. J. Field Robot. **23**(10), 839–861 (2006)
29. MacLellan, M., Patla, A.: Adaptations of walking pattern on a compliant surface to regulate dynamic stability. Exp. Brain Res. **173**, 521–530 (2006)
30. MacLellan, M., Patla, A.: Stepping over an obstacle on a compliant travel surface reveals adaptive and maladaptive changes in locomotion patterns. Exp. Brain Res. **173**, 554–554 (2006)
31. Manjanna, S., Dudek, G., Giguere, P.: Using gait change for terrain sensing by robots. In: International Conference on Computer and Robot Vision (CRV), 2013, pp. 16–22 (2013)
32. Newman, P., Chandran-Ramesh, M., Cole, D., Cummins, M., Harrison, A., Posner, I., Schröter, D.: Describing, navigating and recognising urban spaces – building an end-to-end SLAM system. In: Kaneko, M., Nakamura, Y. (eds.)

ISRR, Springer Tracts in Advanced Robotics, vol. 60, pp. 237–253. Springer (2007)
33. Niwa, T., Inagaki, S., Suzuki, T.: Locomotion control of multi-legged robot based on Follow-the-Contact-Point gait. In: ICCAS-SICE, 2009, pp. 2247–2253 (2009)
34. Ojeda, L., Borenstein, J., Witus, G., Karlsen, R.: Terrain characterization and classification with a mobile robot. J. Field Robot. **23**(2), 103–122 (2006)
35. Palankar, M., Palmer, L.R.: Toward innate leg stability on unmodeled and natural terrain: hexapod walking. In: IROS, pp. 526–531. IEEE (2012)
36. Posner, I., Cummins, M., Newman, P.M.: A generative framework for fast urban labeling using spatial and temporal context. Auton. Robot. **26**(2-3), 153–170 (2009)
37. Sinnet, R., M.P.R.S., Ames, A.D.: A human-inspired hybrid control approach to bipedal robotic walking. In: Proceedings of the 18th World Congress, the International Federation of Automatic Control, pp. 6904–691 1 (2011)
38. Rusu, R.B., Cousins, S.: 3D is here: Point Cloud Library (PCL). In: IEEE International Conference on Robotics and Automation (ICRA). Shanghai, China (2011)
39. Stavens, D., Thrun, S.: A self-supervised terrain roughness estimator for off-road autonomous driving. In: UAI. AUAI Press (2006)
40. Visser, L., Stramigioli, S., Carloni, R.: Control strategy for energy-efficient bipedal walking with variable leg stiffness. In: IEEE International Conference on Robotics and Automation (ICRA), pp. 5624–5629 (2013)
41. Walas, K.: Improving accuracy of local maps with active haptic sensing. In: Kozłowski, K. (ed.) Robot Motion and Control 2011, Lecture Notes in Control and Information Sciences, vol. 422, pp. 137–146. Springer, London (2012)
42. Walas, K.: Tactile sensing for ground classification. J. Autom. Mob. Robot. Int. Syst. **7**(2), 18–23 (2013)
43. Walas, K.: Terrain Classification Using Vision, Depth and Tactile Perception. In: RSS workshop RGB-D: Advanced Reasoning with Depth Cameras., p. Archived on the Website of the Workshop (2013)
44. Walas, K., Belter, D.: Messor – Versatile Walking Robot for Search and Rescue Missions. J. Autom. Mob. Robot. Intell. Syst. **5**(2), 28–34 (2011)
45. Walas, K., Kasinski, A.J.: Discrete event controller for urban obstacles negotiation with walking robot. In: IROS, pp. 181–186. IEEE (2012)
46. Walas, K., Schmidt, A., Kraft, M., Fularz, M.: Hardware implementation of ground classification for a walking robot. In: 9th Workshop on Robot Motion and Control (RoMoCo), 2013, pp. 110–115 (2013)
47. Weiss, C., Frohlich, H., Zell, A.: Vibration-based terrain classification using support vector machines. In: IEEE/RSJ International Conference on Intelligent Robots and Systems, 2006, pp. 4429–4434 (2006)
48. Weiss, C., Tamimi, H., Zell, A.: A combination of vision- and vibration-based terrain classification. In: IEEE/RSJ International Conference on Intelligent Robots and Systems, 2008. IROS 2008, pp. 2204–2209 (2008)
49. Zarrouk, D., Fearing, R.S.: Cost of Locomotion of a Dynamic Hexapedal Robot. In: IEEE International Conference on Robotics and Automation (ICRA), pp. 2533–2538 (2013)
50. Zenker, S., Aksoy, E., Goldschmidt, D., Worgotter, F., Manoonpong, P.: Visual terrain classification for selecting energy efficient gaits of a hexapod robot. In: IEEE/ASME International Conference on Advanced Intelligent Mechatronics (AIM), 2013, pp. 577–584 (2013)